

AIAA 99-2702

Computational Magnetohydrodynamic Model
of a Gasdynamic Mirror Propulsion System

C. J. Ohlandt and K. G. Powell
Department of Aerospace Engineering

T. Kammash
Department of Nuclear Engineering
University of Michigan Ann Arbor, MI

**35th AIAA/ASME/SAE/ASEE Joint Propulsion
Conference and Exhibit
20-24 June 1999
Los Angeles, California**

COMPUTATIONAL MAGNETOHYDRODYNAMIC MODEL OF A GASDYNAMIC MIRROR PROPULSION SYSTEM

Chad J. Ohlandt*, Dept. of Aerospace Engineering
 Terry Kammash†, Dept. of Nuclear Engineering
 Kenneth G. Powell‡, Dept. of Aerospace Engineering
 University of Michigan, Ann Arbor, MI 48109

Abstract

A computational tool for modeling a gasdynamic mirror machine is presented. A gasdynamic mirror is the core of a proposed fusion space propulsion system. The gasdynamic mirror is an axisymmetric magnetic field used to confine a fusion plasma between two magnetic mirrors. The tool is constructed from a full three dimensional, solution adaptive Cartesian grid generator and an ideal magnetohydrodynamic finite volume solution algorithm. The grid generator is fully automated which allows for continual grid adaption around flow characteristics of interest. The solver is based on an MHD Roe approximate flux function due to a symmetrizable form of the equations and combined with an additional embedded magnetic field flux to allow for improved flow solution under conditions where the magnetic energy is much greater than the kinetic energy.

Introduction

In support of the development of gas dynamic mirror (GDM) machines as propulsion systems for interplanetary flight, a computational modeling tool has been developed to corroborate analytical models and to analyze experimental results. In the past, magnetic mirror machines that operate in collisionless regimes have been considered as a possible containment system for terrestrial fusion power plants. However, such work has been largely abandoned due to a number of instabilities found to be present combined with disadvantages of an open ended system. It has been proposed that a higher density gasdynamic version of the mirror machine with a large aspect ratio would have fewer instabilities and make an ideal space propulsion system.[1, 2, 3]

* Graduate Student, Member AIAA

† Professor, Associate Fellow AIAA

‡ Professor, Member AIAA

As experimental work begins to establish proof of concept for the gasdynamic mirror, observations are likely to produce unexpected flow fields or instabilities. Due to the difficulty of taking measurements within a plasma flow field without disturbing it, it will be necessary to numerically model the system to identify the causes of any such anomalies. Additionally, the experimental testing of fusion GDM machines on the scales of tens of meters and hundreds of tons will be difficult and expensive. Computational models will save time, money, and increase safety during development.

The computational tool described in this paper overcomes a number of the challenges with regard to modeling GDM systems. First, a description of the GDM configuration used in this work will be given. Then, a discussion of the grid generation and finite volume methods necessary for modeling it. Finally, validation and the tools capabilities will be explored.

Gasdynamic Mirror

A GDM system is composed of two axisymmetric magnetic mirrors. The magnetic fields of the axisymmetric mirrors can be represented by following equations

$$B_z = B_0 [1 - \alpha \cos(u) I_0(\rho)] \quad (1)$$

$$B_r = B_0 \alpha \sin(u) I_1(\rho) \quad (2)$$

where

$$u = \frac{2\pi z}{L} \quad \rho = \frac{2\pi r}{L} \quad \alpha = \frac{R_m - 1}{R_m + 1}$$

with R_m being the mirror ratio and I_n is a modified Bessel function. This is illustrated in Figure 1.[4]

The gasdynamic regime means that the mean free path is much less than the length of the mirror, $\lambda \ll L$. This reduces the impact of loss cone effects on stability. Additionally, high density near the mirror reduces the likelihood of flute instability. Both are problems that plague traditional mirror fusion devices.

Grid Generation

Initial grids are generated using automated, Cartesian methods, and solution-based adaption allows the code to increase resolution around flow regions of interest during flow solution. The grid is stored in an octree format with the complete domain represented by a single cell which is subdivided into eight children cells. Each of those children cells are then considered parents and subdivided into another eight cells. This continues until a suitable level of resolution is achieved. The initial grid generation employs a curvature test on the geometry within the current cell to determine whether the cell is further subdivided. During the solution of the case, the grid will continue to adapt by further refining cells in regions where the flow has certain characteristics of interest. Current test criteria for solution adaption include velocity gradients ($\nabla \mathbf{v}$), flow vorticity ($\nabla \times \mathbf{v}$), numeric entropy wave strength ($\nabla p - a^2 \nabla \rho$), and current flux ($\nabla \times \mathbf{B}$). Additionally, the grid will be coarsened in areas that do not demonstrate the listed criteria to save memory and reduce the computational load.

Flow Solution

A finite volume conservation formulation is the basis of the MHD solver implemented. Every polygon, either boundary surface or cell interface, is treated like a 1-D Riemann problem. By solving the Riemann problem, the flux across the interface is determined. The iteration method is a multi-stage, explicit time stepping scheme which can be used for steady state or unsteady solutions.

$$\mathbf{U}^{(0)} = \mathbf{U}^n \quad k = 1 \dots m \quad (3)$$

$$\mathbf{U}^{(k)} = \mathbf{U}^{(0)} + \frac{\alpha_k \Delta t}{V_i} \mathbf{R} \left(\mathbf{U}^{(k-1)} \right) \quad (4)$$

$$\mathbf{U}^{(n+1)} = \mathbf{U}^{(m)} \quad (5)$$

where \mathbf{R} , the residual, will be defined shortly.

The ideal MHD equations assume inviscid, continuum flow with conductance occurring on a much smaller time scale as to appear infinite at non-relativistic velocities. The eight resulting equations

include conservation of mass, momentum, magnetic field, and energy.

$$\frac{\partial \rho}{\partial t} + \nabla \cdot (\rho \mathbf{u}) = 0 \quad (6)$$

$$\begin{aligned} \frac{\partial (\rho \mathbf{u})}{\partial t} + \nabla \cdot \left(\rho \mathbf{u} \mathbf{u} + \left(p + \frac{\mathbf{B} \cdot \mathbf{B}}{2\mu_0} \right) \mathbf{I} - \frac{\mathbf{B} \mathbf{B}}{\mu_0} \right) \\ = -\frac{1}{\mu_0} \mathbf{B} \nabla \cdot \mathbf{B} \end{aligned} \quad (7)$$

$$\frac{\partial \mathbf{B}}{\partial t} + \nabla \cdot (\mathbf{u} \mathbf{B} - \mathbf{B} \mathbf{u}) = -\mathbf{u} \nabla \cdot \mathbf{B} \quad (8)$$

$$\begin{aligned} \frac{\partial E}{\partial t} + \nabla \cdot \left[\left(E + p + \frac{\mathbf{B} \cdot \mathbf{B}}{2\mu_0} \right) \mathbf{u} - \frac{1}{\mu_0} (\mathbf{u} \cdot \mathbf{B}) \mathbf{B} \right] \\ = -\frac{1}{\mu_0} (\mathbf{u} \cdot \mathbf{B}) \nabla \cdot \mathbf{B} \end{aligned} \quad (9)$$

The fluxes are calculated using a Roe approximate flux function for the MHD equations. This is possible when the MHD equations are solved in their symmetrizable form as shown below.[5, 6]

$$\frac{\partial \mathbf{U}}{\partial t} + (\nabla \cdot \mathbf{F})^T = \mathbf{S}, \quad (10)$$

$$\mathbf{U} = (\rho, \rho u, \rho v, \rho w, B_x, B_y, B_z, E)^T$$

$$\mathbf{F} = \begin{pmatrix} \rho \mathbf{u} \\ \rho \mathbf{u} \mathbf{u} + \left(p + \frac{\mathbf{B} \cdot \mathbf{B}}{2\mu_0} \right) \mathbf{I} - \mathbf{B} \mathbf{B} \\ \mathbf{u} \mathbf{B} - \mathbf{B} \mathbf{u} \\ \mathbf{u} \left(E + p + \frac{\mathbf{B} \cdot \mathbf{B}}{2\mu_0} \right) - (\mathbf{u} \cdot \mathbf{B}) \mathbf{B} \end{pmatrix}^T \quad (11)$$

$$\mathbf{S} = -\nabla \cdot \mathbf{B} \begin{pmatrix} 0 \\ \mathbf{B} \\ \mathbf{u} \\ \mathbf{u} \cdot \mathbf{B} \end{pmatrix} \quad (12)$$

However, due to the exceedingly large magnetic fields in a GDM system, magnetic terms can dominate the system and small errors in the magnetic field can have profound effects on the wave system modeled by the Roe linearization. Therefore, to increase accuracy, the magnetic field can be separated into two components, a perturbation and the background embedded field.[7]

$$\mathbf{B} = \mathbf{B}_0 + \mathbf{B}_1 \quad \mathbf{U}_1 = (\rho, \rho \mathbf{u}, \mathbf{B}_1, E_1)^T$$

$$E_1 = \frac{p}{\gamma - 1} + \rho \frac{\mathbf{u} \cdot \mathbf{u}}{2} + \frac{\mathbf{B}_1 \cdot \mathbf{B}_1}{2}$$

$$\frac{\partial \mathbf{U}_1}{\partial t} + (\nabla \cdot \mathbf{F}_1)^T + (\nabla \cdot \mathbf{G})^T = \mathbf{S}_1 \quad (13)$$

$$\mathbf{F}_1 = \begin{pmatrix} \rho \mathbf{u} \\ \rho \mathbf{u} \mathbf{u} + (p + \frac{\mathbf{B}_1 \cdot \mathbf{B}_1}{2}) \mathbf{I} - \mathbf{B}_1 \mathbf{B}_1 \\ \mathbf{u} \mathbf{B}_1 - \mathbf{B}_1 \mathbf{u} \\ \mathbf{u} (E_1 + p + \frac{\mathbf{B}_1 \cdot \mathbf{B}_1}{2}) - (\mathbf{u} \cdot \mathbf{B}_1) \mathbf{B}_1 \end{pmatrix}^T \quad (14)$$

$$\mathbf{S}_1 = -\nabla \cdot \mathbf{B}_1 \begin{pmatrix} 0 \\ \mathbf{B} \\ \mathbf{u} \\ \mathbf{u} \cdot \mathbf{B}_1 \end{pmatrix} \quad (15)$$

$$\mathbf{G} = \begin{pmatrix} 0 \\ (\mathbf{B}_0 \cdot \mathbf{B}_1) \mathbf{I} - (\mathbf{B}_0 \mathbf{B}_1 + \mathbf{B}_1 \mathbf{B}_0) \\ \mathbf{u} \mathbf{B}_0 - \mathbf{B}_0 \mathbf{u} \\ (\mathbf{B}_0 \cdot \mathbf{B}_1) \mathbf{u} - (\mathbf{u} \cdot \mathbf{B}_1) \mathbf{B}_0 \end{pmatrix}^T \quad (16)$$

In this form, the Roe approximate flux function retains the identical form as before, except it can no longer be dominated by errors in the full magnetic field. No assumptions were made about the relative sizes of \mathbf{B}_0 and \mathbf{B}_1 . The only requirements are that the embedded field satisfy $\frac{\partial \mathbf{B}_0}{\partial t} = 0$, $\nabla \cdot \mathbf{B}_0 = 0$, and $\nabla \times \mathbf{B}_0 = 0$.

The resulting finite volume formulation would be

$$\begin{aligned} \frac{d\mathbf{U}_i}{dt} V_i + \sum_{faces} \mathbf{F} \cdot \hat{\mathbf{n}} dS + \sum_{faces} \mathbf{G} \cdot \hat{\mathbf{n}} dS \\ = - \begin{pmatrix} 0 \\ \mathbf{B} \\ \mathbf{u} \\ \mathbf{u} \cdot \mathbf{B} \end{pmatrix}_i \sum_{faces} \mathbf{B} \cdot \hat{\mathbf{n}} dS \end{aligned} \quad (17)$$

and the residual term alluded to in the multi-stage update is

$$\begin{aligned} \mathbf{R} = - \begin{pmatrix} 0 \\ \mathbf{B} \\ \mathbf{u} \\ \mathbf{u} \cdot \mathbf{B} \end{pmatrix}_i \sum_{faces} \mathbf{B} \cdot \hat{\mathbf{n}} dS \\ - \sum_{faces} \mathbf{F} \cdot \hat{\mathbf{n}} dS - \sum_{faces} \mathbf{G} \cdot \hat{\mathbf{n}} dS. \end{aligned} \quad (18)$$

Conclusions and Future Work

Validation of the code was done using shock polars and agreed with results in Powell, et al.[7] The computational model produced satisfactory results for low resolution. Some examples of the grid refinement and property profiles can be found in Figures 2, 3, and 4.

However, the large magnetic fields produce extremely fast magneto-acoustic waves. When combined with the high resolution and inversely small cell sizes, it drove the explicit time step to exceedingly small quantities and limits the usefulness of the computational model. This dictates the focus of future work which should be the incorporation of implicit methods. Additional efforts should be made for the inclusion of non-ideal MHD effects such as resistivity and multi-species.

References

- [1] Kammash, T. and Lee, M.-J., "Gasdynamic Fusion Propulsion System for Space Exploration", Journal of Propulsion and Power 11, 3, pp. 544-53, 1995.
- [2] Kammash, T., Lee, M.-J., and Poston, D. I., "High-Thrust-High-Specific Impulse Gasdynamic Fusion Propulsion System", Journal of Propulsion and Power 13, 3, pp. 421-7, 1997.
- [3] Kammash, T. and Galbraith, D. L., "Improved Physics Model for the Gasdynamic Mirror Fusion Propulsion System", Journal of Propulsion and Power 14, 1, pp. 24-8, 1998.
- [4] Post, R. F., "Review Paper: The Magnetic Mirror Approach to Fusion", Nuclear Fusion, 27, 10, pp. 1579-739, 1987.
- [5] Godunov, S. K., "Symmetric Form of the Equations of Magnetohydrodynamics", Numerical Methods for Mechanics of Continuum Medium, 1, pp. 26-34, 1972.
- [6] Powell, K. G., Roe, P. L., Myong, R. S., Gombosi, T. I., and DeZeeuw, D. L., "An Upwind Scheme for Magnetohydrodynamics", AIAA 12th Computational Dynamics Conference, AIAA-95-1704, 1995.
- [7] Powell, K.G., Roe, P. L., Linde, T. J., Gombosi, T. I., and De Zeeuw, D. L., "A Solution-Adaptive Upwind Scheme for Ideal Magnetohydrodynamics", Journal of Computational Physics, revision submitted March 1999.

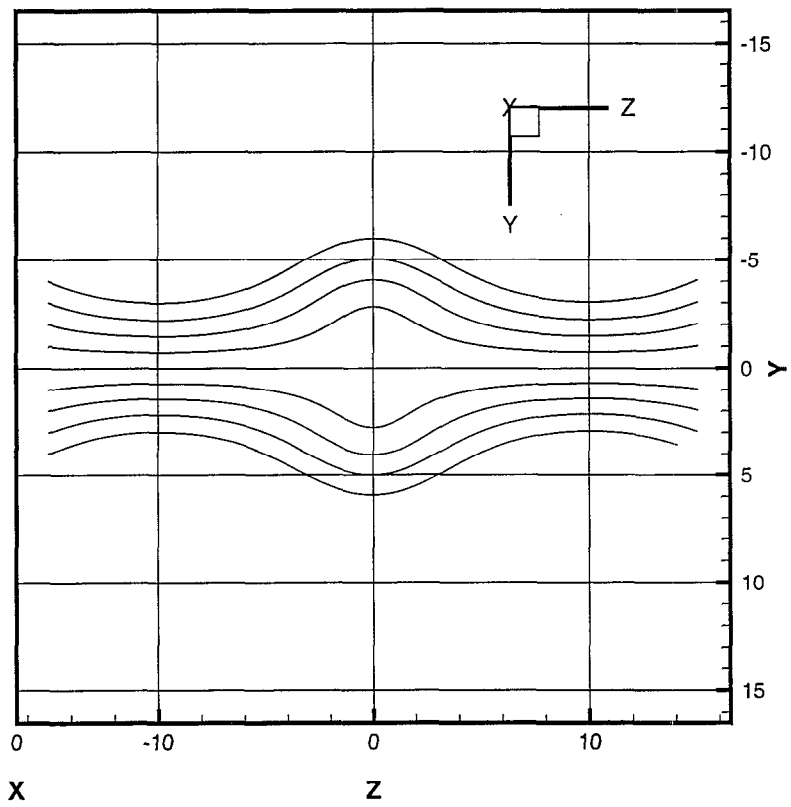


Figure 1: Magnetic field lines for a gasdynamic mirror.

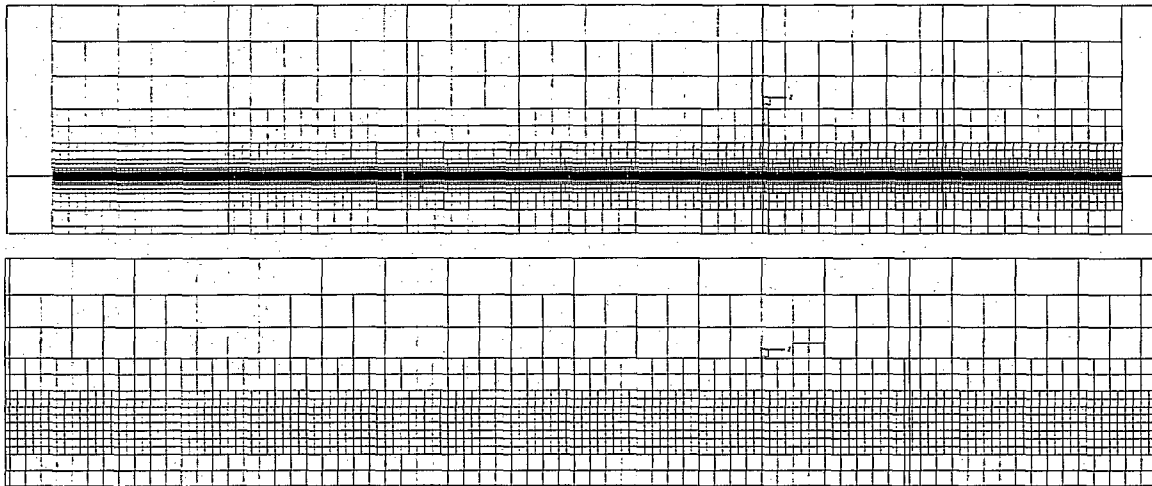


Figure 2: Grids produced by GDM configuration.

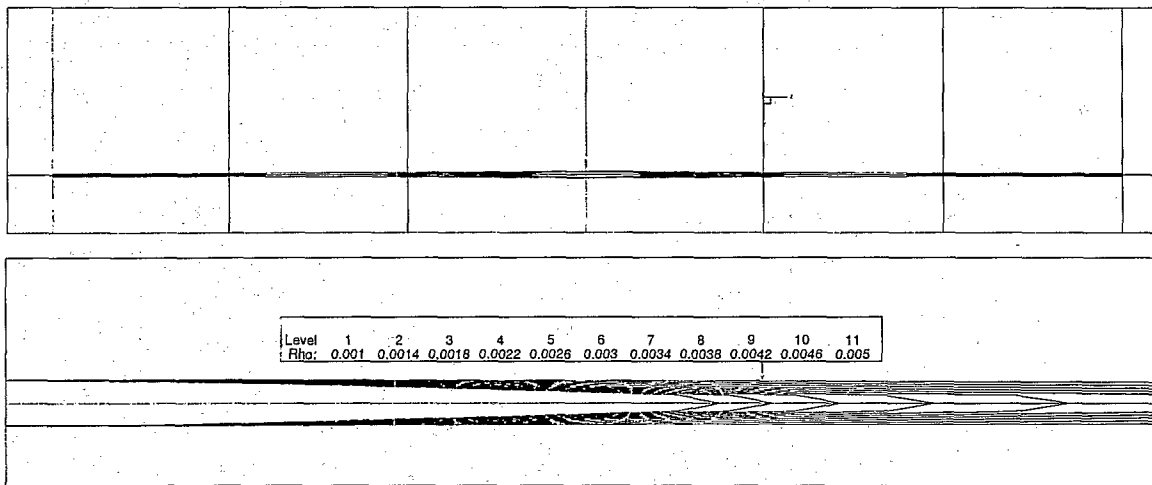


Figure 3: Density profiles.

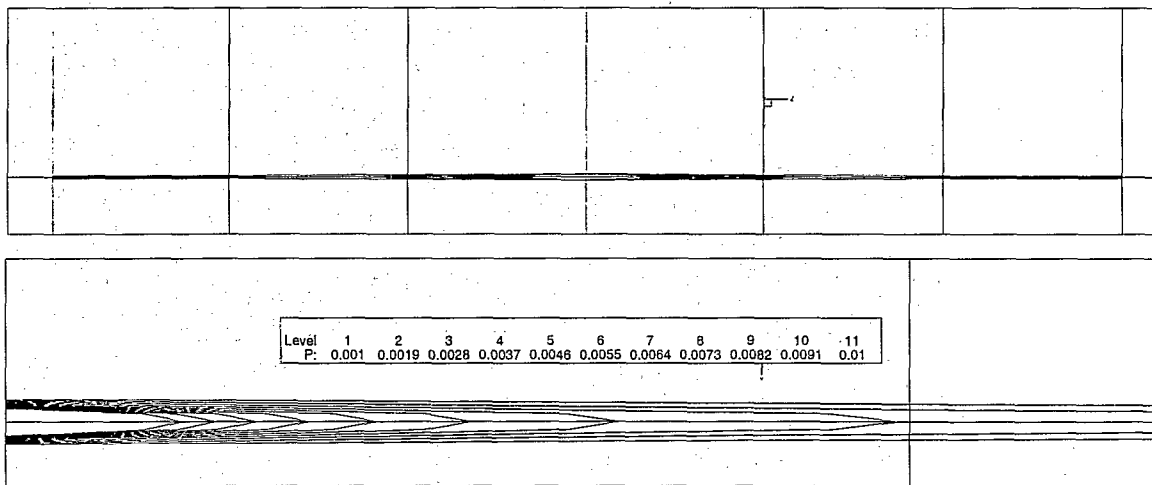


Figure 4: Pressure profiles.